

Incoherent Bi off-centering in $\text{Bi}_2\text{Ti}_2\text{O}_6\text{O}'$ and $\text{Bi}_2\text{Ru}_2\text{O}_6\text{O}'$: Insulator versus metal

Daniel P. Shoemaker*

Materials Science Division, Argonne National Laboratory Argonne, Illinois 60439, USA

Ram Seshadri†

Materials Department, University of California, Santa Barbara, California 93106, USA

Makoto Tachibana‡

National Institute for Materials Science, Namiki 1-1, Tsukuba, Ibaraki 305-0044, Japan

Andrew L. Hector§

School of Chemistry, University of Southampton, Highfield, Southampton SO17 1BJ, United Kingdom

(Received 6 June 2011; revised manuscript received 29 July 2011; published 24 August 2011)

In the cubic, stoichiometric oxide compounds $\text{Bi}_2\text{Ti}_2\text{O}_6\text{O}'$ (also written as $\text{Bi}_2\text{Ti}_2\text{O}_7$) and $\text{Bi}_2\text{Ru}_2\text{O}_6\text{O}'$ (also written as $\text{Bi}_2\text{Ru}_2\text{O}_7$) Bi^{3+} ions on the pyrochlore *A* site display a propensity to off-center. Unlike $\text{Bi}_2\text{Ti}_2\text{O}_6\text{O}'$, $\text{Bi}_2\text{Ru}_2\text{O}_6\text{O}'$ is a metal, so it is of interest to ask whether conduction electrons and/or involvement of Bi *6s* states at the Fermi energy influence Bi^{3+} displacements. The Bi^{3+} off-centering in $\text{Bi}_2\text{Ti}_2\text{O}_6\text{O}'$ has previously been revealed to be incoherent from detailed reverse Monte Carlo analysis of total neutron scattering. Similar analysis of $\text{Bi}_2\text{Ru}_2\text{O}_6\text{O}'$ reveals incoherent off-centering as well, but of smaller magnitude and with distinctly different orientational preference. Analysis of the distributions of metal to oxygen distances presented suggests that Bi in both compounds is entirely Bi^{3+} . Disorder in $\text{Bi}_2\text{Ti}_2\text{O}_6\text{O}'$ has the effect of stabilizing valence while simultaneously satisfying the steric constraint imposed by the presence of the lone pair of electrons. In $\text{Bi}_2\text{Ru}_2\text{O}_6\text{O}'$, off-centering is not required to satisfy valence and seems to be driven by the lone pair. Decreased volume of the lone pair may be a result of partial screening by conduction electrons.

DOI: [10.1103/PhysRevB.84.064117](https://doi.org/10.1103/PhysRevB.84.064117)

PACS number(s): 61.05.fm, 61.43.Bn, 71.30.+h

I. INTRODUCTION

The oxide pyrochlores $A_2B_2O_6O'$, usually abbreviated $A_2B_2O_7$, are well known for their ability to accommodate magnetic cations on interpenetrating sublattices of corner-connected $O'A_4$ tetrahedra and BO_6 octahedra. The geometry of the sublattices often results in magnetically frustrated ground states,^{1,2} resulting in spin-glass, spin-ice, or spin-liquid phases.³ Frustration of concerted atomic displacements (dipolar frustration) has also been proposed, when electronic dipoles rather than magnetic spins are placed on the pyrochlore *A* site,⁴⁻⁶ with the suggested “charge-ice”⁷ displaying the appropriate entropic signatures.⁸ Large atomic displacement parameters associated with the *A*-site cation, seen in Fourier maps of $\text{La}_2\text{Zr}_2\text{O}_7$ ⁹ and in Bi_2M_2O_7 ($B = \text{Ti}, \text{Zn}, \text{Nb}, \text{Ru}, \text{Sn}, \text{Hf}$),¹⁰⁻¹³ contribute to the expanding body of evidence that pyrochlores prefer to accommodate cation off-centering *via* incoherent disorder rather than in ordered noncubic ground states.

Among Bi_2B_2O_7 pyrochlores, $B = \text{Ti}, (\text{Zn}/\text{Nb}), \text{Sn}$, and Hf are insulators, while $B = \text{Ru}, \text{Rh}, \text{Ir}$, and Pt are metals.¹⁴ The behavior of Bi^{3+} is suggested to be quite different in insulating and metallic pyrochlores. In insulating $\text{Bi}_2\text{Ti}_2\text{O}_6\text{O}'$ and $\text{Bi}_2\text{Sn}_2\text{O}_7$ (cubic above 920 K) the Bi is offset by ~ 0.4 Å from the ideal site. This Bi off-centering is aperiodic but otherwise analogous to the *correlated* motion of lone-pair active Bi^{3+} in the ionic conductor Bi_2O_3 ¹⁵ or multiferroic BiFeO_3 .¹⁶ In metallic pyrochlores, the suggestion is that weaker *A*-*O'* interactions preclude any displacement at all.¹⁷⁻¹⁹ However, Rietveld refinements for compounds where $B = \text{Ru}, \text{Rh}$, and Ir show that Bi off-centering is still present in experiment.^{10,20-22}

The short-range correlation of Bi displacements has been probed using reverse Monte Carlo modeling of the diffuse streaks in electron diffraction patterns.²³

In this contribution, we compare structural details in insulating $\text{Bi}_2\text{Ti}_2\text{O}_6\text{O}'$ and metallic $\text{Bi}_2\text{Ru}_2\text{O}_6\text{O}'$ using pair distribution function (PDF) analysis with least-squares and reverse Monte Carlo (RMC) modeling. These techniques reveal the precise structural tendencies of Bi^{3+} off-centering, even in the case of incoherent ice-like disorder.⁶ Specific details of bond distances, angles, and real-space shapes can be extracted from the RMC model because it is predicated on fits to the atom-atom distances in the PDF. The work should be placed in the context of ionic off-centering in metallic systems and the screening of ferroelectric dipoles, as first suggested by Anderson and Blount,²⁵ which finds application in the context of heavily doped perovskite titanates.²⁶ We find that the large displacements in $\text{Bi}_2\text{Ti}_2\text{O}_6\text{O}'$ can be reconciled with bond-valence analysis, but displacements in $\text{Bi}_2\text{Ru}_2\text{O}_6\text{O}'$ are not driven by valence considerations alone.

To introduce the comparison, Fig. 1 shows that the scaled heat capacities of $\text{Bi}_2\text{Ti}_2\text{O}_6\text{O}'$ and $\text{Bi}_2\text{Ru}_2\text{O}_6\text{O}'$ display pronounced low-temperature humps in plots of C/T^3 vs T that are indicative of local Einstein modes, suggestive of glassy disorder. This large local-mode contribution is largely absent in $\text{Y}_2\text{Ti}_2\text{O}_7$, which has no lone pair and no experimentally resolvable displacive disorder.⁸ Disorder on the *O'*/ Bi_4 sublattice is also seen in the average structure Rietveld refinement of Bragg neutron scattering, masquerading as very large atomic displacement parameters (ADPs) on the Bi sites, displayed as 95% ellipsoids in Fig. 1.

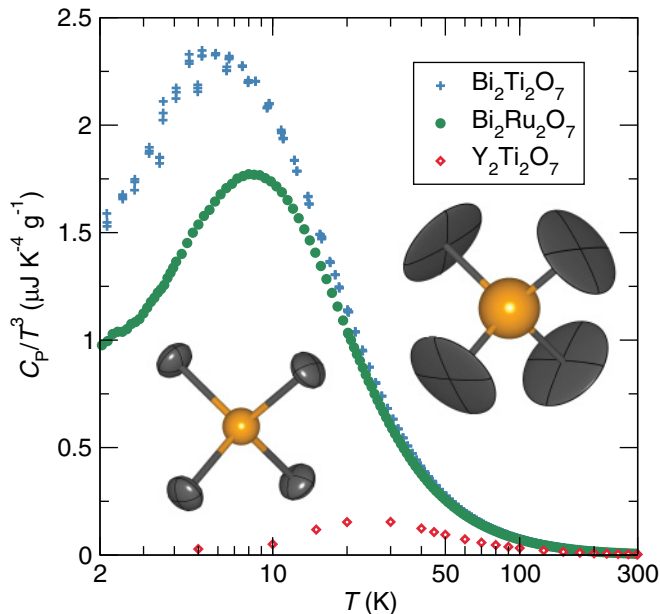


FIG. 1. (Color online) Heat capacities of three pyrochlores show a strong dependence on the magnitude of static A -site disorder (large in $\text{Bi}_2\text{Ti}_2\text{O}_6\text{O}'$, present in $\text{Bi}_2\text{Ru}_2\text{O}_6\text{O}'$, and none in $\text{Y}_2\text{Ti}_2\text{O}_7$). Note that the electronic contribution to the heat capacity of $\text{Bi}_2\text{Ru}_2\text{O}_6\text{O}'$ has been subtracted. The results of Rietveld refinement of Bragg neutron scattering, displayed as 95% ellipsoids on O' (orange/gray) and Bi (black) on $\text{Bi}_2\text{Ru}_2\text{O}_6\text{O}'$ (left) and $\text{Bi}_2\text{Ti}_2\text{O}_6\text{O}'$ (right), point to static Bi^{3+} disorder being enveloped within the large disks. Data are adapted from Refs. 8, 22, and 24.

II. METHODS

Preparation and average structure analysis of the $\text{Bi}_2\text{Ti}_2\text{O}_6\text{O}'$ powder used in this study has been reported by Hector and Wiggin.¹¹ $\text{Bi}_2\text{Ru}_2\text{O}_6\text{O}'$ was prepared as single crystals by Tachibana²² and finely ground prior to measurement. Time-of-flight (TOF) neutron powder diffraction was collected at the NPDF instrument at the Los Alamos National Laboratory at 298 and 14 K. Rietveld refinement made use of the GSAS code.²⁷ Extraction of the PDF with PDFGETN²⁸ used $Q_{\text{max}} = 35 \text{ \AA}^{-1}$. Reverse Monte Carlo simulations were run using RMCPROFILE version 6.²⁹ All atoms move freely in RMC simulations, and while hard-sphere cutoffs were applied, no clustering of atoms at these nearest-neighbor distances occurred. Electronic densities of states (DOS) were calculated by the linear muffin-tin orbital method within the atomic sphere approximation using version 47C of the Stuttgart TB-LMTO-ASA program.³⁰ Bond-valence sums (BVS) were extracted from the RMC supercell as described in previous work on CuMn_2O_4 ,³¹ using the R_0 values of Brese and O'Keeffe.³²

III. RESULTS AND DISCUSSION

The total DOS for $\text{Bi}_2\text{Ti}_2\text{O}_6\text{O}'$ and $\text{Bi}_2\text{Ru}_2\text{O}_6\text{O}'$ are shown in Fig. 2(a). The features are similar, with metallic $\text{Bi}_2\text{Ru}_2\text{O}_6\text{O}'$ shifted in a nearly rigid-band fashion by approximately 2 eV downward, in agreement with previous work.¹⁸ Partial Bi s and p DOS are shown in Fig. 2(b). In both cases, some Bi s states are present at the top of the filled Bi p and Bd bands. Bi s states

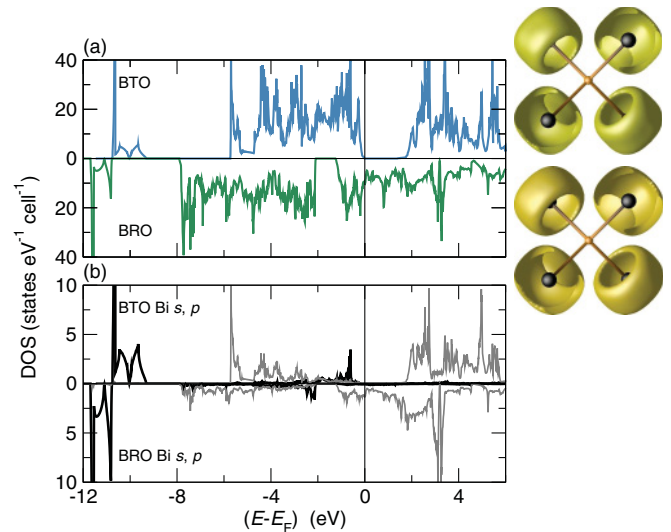


FIG. 2. (Color online) (a,b) The computed total densities of states (DOS) for $\text{Bi}_2\text{Ti}_2\text{O}_6\text{O}'$ and $\text{Bi}_2\text{Ru}_2\text{O}_6\text{O}'$. Below, Bi s (dark) and p (light) states are shown. Electron localization functions (ELFs) for both compounds are shown on the right side as gold (gray) lobes around black Bi ions. Both ideal structures show annuli of lone pairs around Bi ions.

are plotted as electron localization functions ($\text{ELF} \approx 0.65$) isosurfaces at the right of Figs. 2(a) and 2(b). With Bi in their ideal $16c$ positions, the ELFs both show essentially identical circularly averaged lone pairs.⁷ Assuming similar lone pair-cation distances, the ELFs imply that both compounds should have the same cation displacement in the real ground-state structures.

Time-of-flight neutron diffraction Rietveld refinements at $T = 14 \text{ K}$ and 300 K were performed using the ideal pyrochlore model with Bi on the $16c$ sites and anisotropic ADPs. Fits at 14 K are shown in Fig. 3. No substantial differences were found from the analysis of Hector and Wiggin¹¹ or Tachibana *et al.*,²² including the occupancy: stoichiometric $\text{Bi}_2\text{Ti}_2\text{O}_6\text{O}'$ and a Bi occupancy of 0.97 for $\text{Bi}_2\text{Ru}_2\text{O}_6\text{O}'$. The ADPs from 14 K Rietveld refinement are displayed as 95% ellipsoids in Fig. 1. The most apparent difference is the larger, disk-shaped ellipsoid representing Bi in $\text{Bi}_2\text{Ti}_2\text{O}_6\text{O}'$. Bi is known to be off-centered from the ideal $16c$ position in a ring normal to the $\text{O}'\text{-Bi-O}'$ bond.^{6,11,33} The large anisotropic ADPs of Bi envelop this ring. A split Bi position can give a better fit to the diffraction data. The previous study found that there is a slight tendency for Bi to prefer the $96h$ positions.⁶ This represents a sixfold splitting of the Bi into sites that are displaced $\sim 0.4 \text{ \AA}$ from the ideal site and pointing *between* nearby O ions on $48f$ sites. Bi ADPs in $\text{Bi}_2\text{Ru}_2\text{O}_6\text{O}'$ also suggest displacive disorder. They too are anisotropic and appear as slightly flattened ellipses in Fig. 1.

The most straightforward way to compare the Rietveld-refined unit cell with the local structure is via least-squares PDF refinements, shown in Fig. 4. Two issues should be considered. First, the fit for $\text{Bi}_2\text{Ti}_2\text{O}_6\text{O}'$ is significantly worse overall than $\text{Bi}_2\text{Ru}_2\text{O}_6\text{O}'$. This implies that the local structure of $\text{Bi}_2\text{Ti}_2\text{O}_6\text{O}'$ is more poorly described by the $Fd\bar{3}m$ unit cell. Second, the fit for $\text{Bi}_2\text{Ti}_2\text{O}_6\text{O}'$ is poorest at low r , which contains details of near-neighbor atomic distances

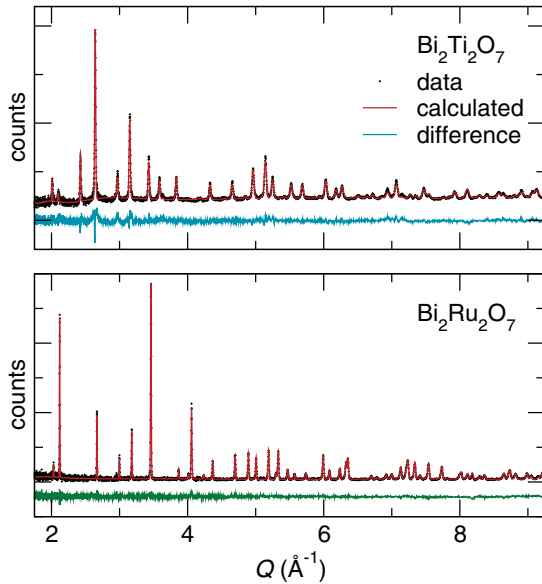


FIG. 3. (Color online) Time-of-flight neutron diffraction Rietveld refinement of (top) $\text{Bi}_2\text{Ti}_2\text{O}_6\text{O}'$ and (bottom) $\text{Bi}_2\text{Ru}_2\text{O}_6\text{O}'$ at 14 K using the ideal pyrochlore structure with anisotropic thermal parameters. The fit to $\text{Bi}_2\text{Ti}_2\text{O}_6\text{O}'$ is visibly worse due to large amounts of diffuse scattering intensity. This diffuse scattering is a result of large local Bi and O' displacements.

(of particular importance are Bi-O and Bi-O'), and is still unsatisfactory at higher r , even though a larger number of pairs are being included. The fit for $\text{Bi}_2\text{Ru}_2\text{O}_6\text{O}'$ is equally decent at all r values up to 20 Å.

These PDF fits do not give the positions of atoms in either compound, but they quickly reveal valuable information about

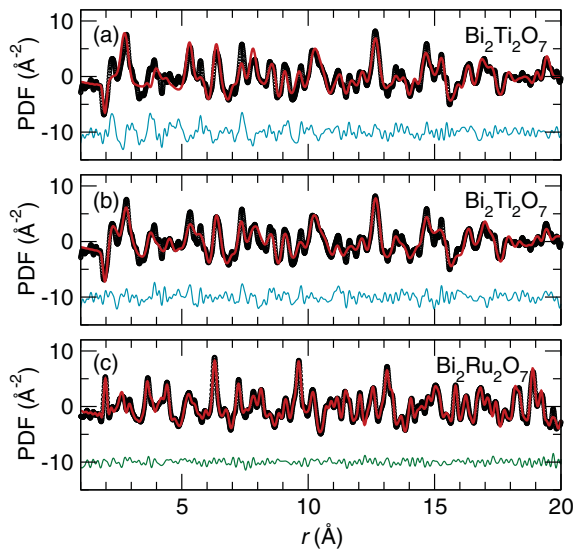


FIG. 4. (Color online) Least-squares PDF fits (using the unit cell from Rietveld refinement) do not reproduce the low- r structure of $\text{Bi}_2\text{Ti}_2\text{O}_6\text{O}'$ due to the inability of a unit-cell-based description to accommodate incoherent static displacements. Bi are placed on $8a$ sites in (a) and on split $96h$ sites in (b). Both descriptions give worse agreement than the fit to $\text{Bi}_2\text{Ru}_2\text{O}_6\text{O}'$ in (c), using $8a$ sites, which is significantly better because the static displacements are smaller.

the presence of local atomic displacements (more apparent in $\text{Bi}_2\text{Ti}_2\text{O}_6\text{O}'$ than $\text{Bi}_2\text{Ru}_2\text{O}_6\text{O}'$) and the correlations between them (still unable to be averaged for $r < 20$ Å). Extracting structural tendencies of geometrically frustrated compounds via least-squares refinement is inherently difficult because there is no straightforward way to model the large, complex collection of discrete displacements needed to reproduce the disorder. Least squares is not a suitable algorithm for determining so many free Bi positions (scales linearly with supercell volume), especially when their interactions may be correlated. Instead, we remove symmetry constraints and use RMC to investigate how Bi are distributed within a large supercell.

Simulations were carried out using the RMC method to investigate the precise positions of Bi. Simultaneous fits to the PDF and Bragg profile for $\text{Bi}_2\text{Ru}_2\text{O}_6\text{O}'$ are shown in Fig. 5. Unit-cell-based modeling (least-squares refinements, including Rietveld) usually fails to model incoherent static displacements. In contrast, each RMC supercell contains thousands of ions of each type. Folding the RMC supercell into a single unit cell produces “point clouds” of ions at each crystallographic site. These clouds display the propensity of ions to displace from their ideal positions. The mean-squared displacement of points is in quantitative agreement with the average ADPs obtained from Rietveld refinement. Mapping these points as two-dimensional histograms (Fig. 6) shows the tendency of Bi nuclei to offset in $\text{Bi}_2\text{Ti}_2\text{O}_6\text{O}'$ and $\text{Bi}_2\text{Ru}_2\text{O}_6\text{O}'$. The Bi clouds are viewed along the O'-Bi-O' bond [Fig. 6(a), top] and perpendicular [Fig. 6(a), bottom] for two temperatures.

The Bi ring in $\text{Bi}_2\text{Ti}_2\text{O}_6\text{O}'$ is evident from Fig. 6 and has a diameter of ~ 0.8 Å. At 300 K, the ring is more diffuse. We attribute this to thermal broadening. Interestingly, the ring is not a perfect circle. It has a sixfold symmetry corresponding to the preference for Bi to occupy the $96h$ positions (corners of the hexagon), which point between the six neighboring $48f$ O ions in the TiO_6 network.⁶

The Bi distribution in $\text{Bi}_2\text{Ru}_2\text{O}_6\text{O}'$ is distinctly different, but static displacement is still present. The displacements are densely clustered close to the ideal position, and there is no

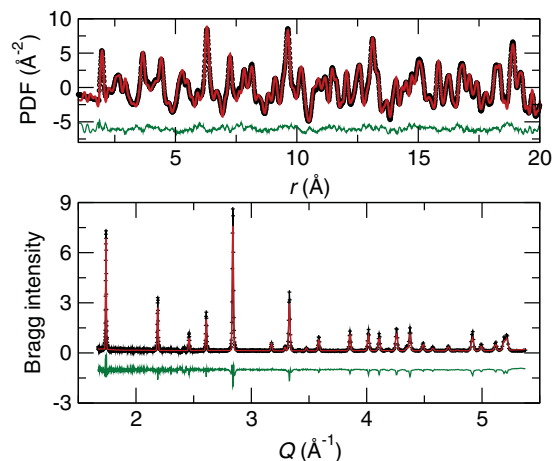


FIG. 5. (Color online) RMC fits to the PDF and Bragg profile of $\text{Bi}_2\text{Ru}_2\text{O}_6\text{O}'$ at 14 K constrain the local structure (atom-atom distances) and long-range periodicity (cell parameter, ADPs)

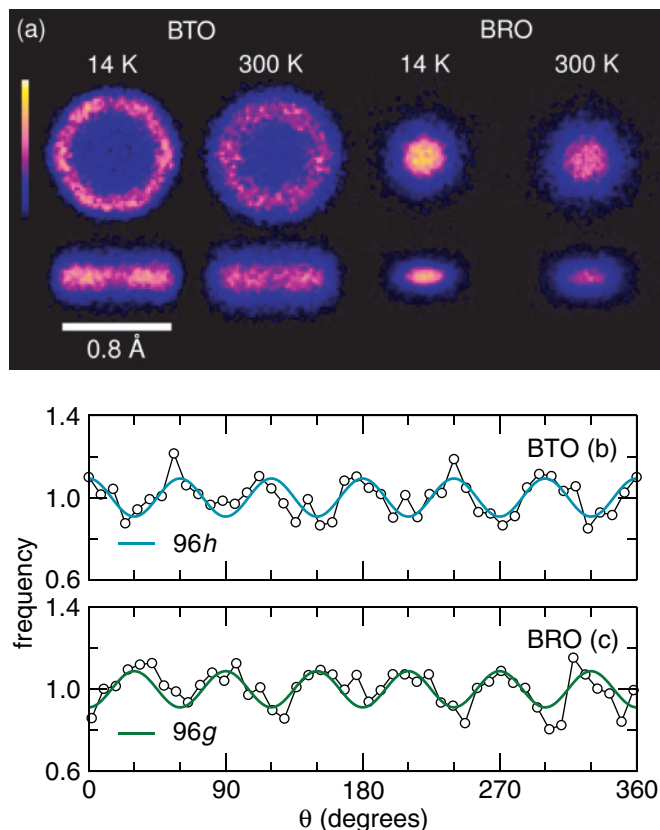


FIG. 6. (Color online) (a) Clouds of Bi nuclear intensity for $\text{Bi}_2\text{Ti}_2\text{O}_6\text{O}'$ and $\text{Bi}_2\text{Ru}_2\text{O}_6\text{O}'$ are viewed along (top) and normal to (bottom) the $\text{O}'\text{-Bi-O}'$ bond. Static disorder in both produces hexagonal ring or disk shapes centered on the ideal position. (b) and (c) Distribution of Ti and Ru as a function of angle around the ring θ . The sixfold modulations indicate a preference for 96*h* and 96*g* sites. Data in (b) are adapted from Ref. 6.

hollow center as in $\text{Bi}_2\text{Ti}_2\text{O}_6\text{O}'$. However, the perpendicular view reveals that the Bi distribution is still disk shaped. Most surprising is the symmetry of the disk. It also has a hexagonal shape, but the hexagon is rotated 30° with respect to what is seen in $\text{Bi}_2\text{Ti}_2\text{O}_6\text{O}'$, with flat edges on the left and right and corners on the top and bottom. This implies that Bi is displacing *toward* the nearby $48f$ O onto 96*g* positions. The Bi offset roughly agrees with the value of 0.16 \AA found in the split-site model of Avdeev.¹⁰

Quantitative RMC Bi nuclear density as a function of the angle θ around a ring normal to the $\text{O}'\text{-Bi-O}'$ bonds is shown in Figs. 6(b) and 6(c). Both compounds show sixfold modulation fit by a cosine curve with a period of 60° , but their oscillations are offset by 30° .

Bond-valence sums are calculated for each individual cation in the supercell and are plotted as histograms in Fig. 7(a) for $\text{Bi}_2\text{Ti}_2\text{O}_6\text{O}'$ and Fig. 7(b) for $\text{Bi}_2\text{Ru}_2\text{O}_6\text{O}'$ at $T = 14$ and 300 K. In all cases, BVS distributions are centered on the expected valence: Bi^{3+} , Ti^{4+} , Ru^{4+} , and O^{2-} . A slight sharpening is seen for the low-temperature measurement. These distributions reveal that the RMC simulations contain chemically reasonable bond lengths despite the absence of such distance constraints in the simulations. They also reveal that there is no tendency for Bi^{5+} in $\text{Bi}_2\text{Ru}_2\text{O}_6\text{O}'$, supporting

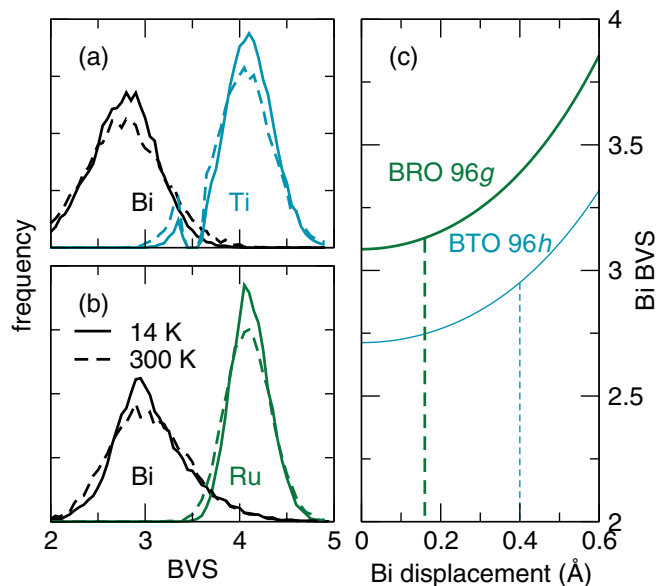


FIG. 7. (Color online) Bond-valence sums (BVS) extracted from the RMC supercells show entirely Bi^{3+} in (a) $\text{Bi}_2\text{Ti}_2\text{O}_6\text{O}'$ and (b) $\text{Bi}_2\text{Ru}_2\text{O}_6\text{O}'$. The small shoulder of Ti^{3+} is a consequence of peak broadening. Only Ti^{4+} (note peak center) exists in the sample. (c) Bi BVS is plotted as a function of displacement into 96*g* and 96*h* positions. $\text{Bi}_2\text{Ti}_2\text{O}_6\text{O}'$ requires significant off-centering to obtain valence from $48f$ O anions. Dashed lines show the actual displacement and BVS.

the conclusion from LMTO calculations that Bi $5s$ states are localized far below the Fermi energy.

The calculated Bi BVS versus displacement in Fig. 7(c) demonstrates why displacements are more pronounced in $\text{Bi}_2\text{Ti}_2\text{O}_6\text{O}'$. In the average structures, $\text{Bi}_2\text{Ti}_2\text{O}_6\text{O}'$ and $\text{Bi}_2\text{Ru}_2\text{O}_6\text{O}'$ respectively obtain only $1.31+$ and $1.38+$ per Bi from bonds to O' . The majority of the valence is obtained from $48f$ O and increases with Bi displacement, represented by the upward curve. Bi in both compounds gain about the same valence from $48f$ O, but a large displacement is required to reach the retracted Ti_2O_6 sublattice. The result is that each Bi in $\text{Bi}_2\text{Ti}_2\text{O}_6\text{O}'$ gains an uneven amount of charge from the six $48f$ O, locking in dipoles. This explains why the Bi displacements appear to be static in variable temperature measurements.⁶ The rigidity of the $B_2\text{O}_6$ sublattice is confirmed by small ADPs on $48f$ O in both compounds, even in the presence of nearby Bi off-centering. In $\text{Bi}_2\text{Ru}_2\text{O}_6\text{O}'$, the Ru_2O_6 network pushes $48f$ O closer to Bi so that valence is satisfied.

We have considered whether covalency could lead to difficulties in using BVS to judge valence in $\text{Bi}_2\text{Ru}_2\text{O}_6\text{O}'$: should more covalent bonding (shorter $M\text{-O}$ bonds) lead to Bi and Ru requiring *more* than the formal $3+$ and $4+$ to be satisfied? This seems unlikely, not only because Rietveld refinement and RMC find the desired states centered near the nominal values. The average structure of semi-conducting $\text{BiCaRu}_2\text{O}_7$ ³⁴ displays much higher BVS sums ($3.25+$ for Bi and $4.20+$ for Ru) than $\text{Bi}_2\text{Ru}_2\text{O}_6\text{O}'$, but large anisotropic ADPs on the A site portend static disorder nonetheless.

In $\text{Bi}_2\text{Ti}_2\text{O}_6\text{O}'$, off-centering helps satisfy Bi valence, and the lone pair can be accommodated in the opposite direction. In $\text{Bi}_2\text{Ru}_2\text{O}_6\text{O}'$, no off-centering is necessary from valence considerations, so static disorder may be driven by lone-pair activity. Metallic screening in $\text{Bi}_2\text{Ru}_2\text{O}_6\text{O}'$ is expected to decrease repulsions of the lone pair from nearby O,²¹ allowing Bi to stay closer to the ideal position than the traditional cation–lone pair distance would dictate. This is supported by the idea that lone pairs often exhibit decreased volumes.³⁵

IV. CONCLUSIONS

In conclusion, reverse Monte Carlo structural analysis using total neutron scattering provides a detailed view of the incoherent static displacements in $\text{Bi}_2\text{Ti}_2\text{O}_6\text{O}'$ and $\text{Bi}_2\text{Ru}_2\text{O}_6\text{O}'$. Real-space maps of static displacements reveal the distinct magnitudes and directions of Bi off-centering in $\text{Bi}_2\text{Ti}_2\text{O}_6\text{O}'$ and $\text{Bi}_2\text{Ru}_2\text{O}_6\text{O}'$. While static displacements in the insulator $\text{Bi}_2\text{Ti}_2\text{O}_6\text{O}'$ can be understood on the basis of valence satisfaction alone, the cause for displacements in metallic $\text{Bi}_2\text{Ru}_2\text{O}_6\text{O}'$ is not captured by first-principles calculations on the ideal compound or by the bond-valence sum. As a result, we propose that an incoherent lone-pair-driven distortion is

present, with smaller off-centering distance due to partial screening by conduction electrons.

ACKNOWLEDGMENTS

We thank Anna Llobet, Thomas Proffen, Joan Siewenie, Katharine Page, and Graham King for helpful discussions and their hospitality while D.P.S. was visiting the Lujan Center. This work utilized NPDF at the Lujan Center at the Los Alamos Neutron Science Center, funded by the DOE Office of Basic Energy Sciences and operated by Los Alamos National Security LLC under DOE Contract No. DE-AC52-06NA25396. Simulations were performed on the Hewlett Packard QSR cluster at the California NanoSystems Institute. The UCSB-LANL Institute for Multiscale Materials Studies, the National Science Foundation (Grant No. DMR 0449354), and the use of MRL Central Facilities, supported by the MRSEC Program of the NSF (Grant No. DMR05-20415), a member of the NSF-funded Materials Research Facilities Network (<http://www.mrfn.org>), are gratefully acknowledged. Work at Argonne National Laboratory is supported by UChicago Argonne, a US DOE Office of Science Laboratory, operated under Contract No. DE-AC02-06CH11357.

*dshoemaker@anl.gov

†seshadri@mrl.ucsb.edu

‡tachibana.makoto@nims.go.jp

§a.l.hector@soton.ac.uk

¹A. P. Ramirez, *Annu. Rev. Mater. Sci.* **24**, 453 (1994).

²A. P. Ramirez, A. Hayashi, R. J. Cava, R. Siddharthan, and B. S. Shastry, *Nature (London)* **399**, 333 (1999).

³B. Canals and C. Lacroix, *Phys. Rev. Lett.* **80**, 2933 (1998).

⁴B. Melot, E. Rodriguez, T. Proffen, M. Hayward, and R. Seshadri, *Mater. Res. Bull.* **41**, 961 (2006).

⁵T. M. McQueen, D. V. West, B. Muegge, Q. Huang, K. Noble, H. W. Zandbergen, and R. J. Cava, *J. Phys. Condens. Matter* **20**, 235210 (2008).

⁶D. P. Shoemaker, R. Seshadri, A. L. Hector, A. Llobet, T. Proffen, and C. J. Fennie, *Phys. Rev. B* **81**, 144113 (2010).

⁷R. Seshadri, *Solid State Sci.* **8**, 259 (2006).

⁸B. C. Melot, R. Tackett, J. O'Brien, A. L. Hector, G. Lawes, R. Seshadri, and A. P. Ramirez, *Phys. Rev. B* **79**, 224111 (2009).

⁹Y. Tabira, R. L. Withers, T. Yamada, and N. Ishizawa, *Z. Kristallogr.* **216**, 92 (2001).

¹⁰M. Avdeev, M. K. Haas, J. D. Jorgensen, and R. J. Cava, *J. Solid State Chem.* **169**, 24 (2002).

¹¹A. L. Hector and S. B. Wiggin, *J. Solid State Chem.* **177**, 139 (2004).

¹²T. A. Vanderah, I. Levin, and M. W. Lufaso, *Eur. J. Inorg. Chem.* **2005**, 2895 (2005).

¹³S. J. Henderson, O. Shebanova, A. L. Hector, P. F. McMillan, and M. T. Weller, *Chem. Mater.* **19**, 1712 (2007).

¹⁴M. A. Subramanian, G. Aravamudan, and G. V. S. Rao, *Prog. Solid State Chem.* **15**, 55 (1983).

¹⁵S. T. Norberg, S. G. Eriksson, and S. Hull, *Solid State Ionics* (2010).

¹⁶N. A. Hill, *Annu. Rev. Mater. Res.* **32**, 1 (2002).

¹⁷A. Walsh, G. W. Watson, D. J. Payne, R. G. Edgell, J. Guo, P. A. Glans, T. Learmonth, and K. E. Smith, *Phys. Rev. B* **73**, 235104 (2006).

¹⁸B. B. Hinojosa, J. C. Nino, and A. Asthagiri, *Phys. Rev. B* **77**, 104123 (2008).

¹⁹B. B. Hinojosa, P. M. Lang, and A. Asthagiri, *J. Solid State Chem.* **183**, 262 (2010).

²⁰B. J. Kennedy, *J. Solid State Chem.* **123**, 14 (1996).

²¹B. J. Kennedy, *Mater. Res. Bull.* **32**, 479 (1997).

²²M. Tachibana, Y. Kohama, T. Shimoyama, A. Harada, T. Taniyama, M. Itoh, H. Kawaji, and T. Atake, *Phys. Rev. B* **73**, 193107 (2006).

²³A. L. Goodwin, R. L. Withers, and H. Nguyen, *J. Phys. Condens. Matter* **19**, 335216 (2007).

²⁴M. B. Johnson, D. D. James, A. Bourque, H. A. Dabkowska, B. D. Gaulin, and M. A. White, *J. Solid State Chem.* **182**, 725 (2009).

²⁵P. W. Anderson and E. I. Blount, *Phys. Rev. Lett.* **14**, 217 (1965).

²⁶K. Page, T. Kolodiaznyi, T. Proffen, A. K. Cheetham, and R. Seshadri, *Phys. Rev. Lett.* **101**, 205502 (2008).

²⁷A. Larson and R. Von Dreele, Los Alamos National Laboratory, Report No. LAUR 86-748, 2000 (unpublished).

²⁸P. F. Peterson, M. Gutmann, T. Proffen, and S. J. L. Billinge, *J. Appl. Crystallogr.* **33**, 1192 (2000).

²⁹M. G. Tucker, D. A. Keen, M. T. Dove, A. L. Goodwin, and Q. Hui, *J. Phys. Condens. Matter* **19**, 335218 (2007).

- ³⁰O. Jepsen and O. K. Andersen, Max-Planck Institut für Festkörperforschung, Stuttgart, Germany (2000) [<http://www.fkf.mpg.de/andersen/>].
- ³¹D. P. Shoemaker, J. Li, and R. Seshadri, *J. Am. Chem. Soc.* **131**, 11450 (2009).
- ³²N. E. Brese and M. O'Keeffe, *Acta Crystallogr., Sect. B* **47**, 192 (1991).
- ³³I. Radosavljevic, J. S. O. Evans, and A. W. Sleight, *J. Solid State Chem.* **136**, 63 (1998).
- ³⁴B. J. Kennedy, *J. Solid State Chem.* **119**, 254 (1995).
- ³⁵M. W. Stoltzfus, P. M. Woodward, R. Seshadri, J. Klepser, and B. Bursten, *Inorg. Chem.* **46**, 3839 (2007).